**Proceedings of the ECCOMAS Thematic International Conference on
Simulation and Modeling of Biological Flows (SIMBIO 2011)
September 21-23, 2011, VUB, Brussels, Belgium**

Spectral relevance of glottal jet interaction with supraglottal structures

Christoph Brücker, Michael Triep, Willy Mattheus , Rüdiger Schwarze

Institute of Mechanics and Fluid Dynamics (IMFD),
TU Bergakademie Freiberg
Lampadiusstrasse 4, 09596, Freiberg, Germany,
bruecker@imfd.tu-freiberg.de

Abstract
The details in the formation of the acoustic source spectrum in voice production during phonation are not yet fully understood. Part of the acoustic spectrum is due to vortex-induced sound generated by the glottal jet flow interacting with the walls in the supraglottal space. This interaction depends on the glottal jet dynamics and the physiological geometry. A driven mechanical model of the vocal folds is used with the aim to study the jet dynamics including the interaction with the ventricular folds, which form a second supraglottal constriction. Numerical simulations of the 3D unsteady flow within the glottal region are carried out. The results show topological characteristics of the glottal jet flow which are in good agreement with earlier flow visualization. When the prominent ventricular folds are included in the glottal flow channel the jet evolves differently due to the interaction with these supraglottal structures. This leads to a changed distribution and abundance of the vortex-induced acoustic sources and changed spectral properties of the flow close to the glottis.

Keywords: glottal jet flow, jet instability, ventricular folds.

Introduction
During human phonation a jet emerges and decays periodically downstream the dynamic gap between both vocal folds named the glottis. In addition, immediately downstream of the glottis the developing jet interacts with supraglottal structures such as the laryngeal walls. This flow-structure interaction depends on the oscillatory motion of the vocal folds and the anatomical situation in the supraglottic space, which is specific for each individual. Irregular oscillations of the vocal folds can lead to a vectoring of the pulsating jet and therefore may trigger stronger jet-wall interactions as in regular oscillatory motion. In literature several studies on free and confined jets, including pulsating ones, can be found. Only few references of confined jets in channels with systematic variation of wall-geometry are reported.

Of special interest in human phonation is a second constriction built by the so called ventricular vocal folds (also named the false focal folds). This second constriction also forms a cavity with the downstream face of the glottis, which is the Morgagni's ventricle. The effect on the glottal jet flow from simplified false folds configurations downstream of the vocal folds has been already partly studied by different authors [1]-[5], but their effect on the spectral content of acoustically relevant vortex dynamics is still not fully understood. Furthermore, most of these studies were based on highly simplified 2D orifice geometries of the glottal gap, thus ignoring any 3D effects of jet-evolution downstream. Instead, the physiological glottis evidences a 3D orifice shape similar to a lens-like hull-shape and shows a complex kinematics of the gap contour changing from a converging opening to a divergent closing phase. These aforementioned effects are included in our model using a driven mechanical model with two counter-rotating cams as introduced by [5].

The present paper studies the influence of the dynamical changing glottal orifice and the ventricular folds upon the instabilities of the glottal jet issuing a symmetric opening. The influence of prominent ventricular folds upon the jet edge instabilities are in the focus of the present work. The jet issues a quasi-elliptic lens-like orifice of aspect ratio 6 into a confined test channel. The downstream parameters influencing the glottal jet include the position of the second constriction with regard to the glottis, the size and shape of the cavity and the false folds and the action of the latter. Depending on the size of the cavity and the instant of the cycle, the glottal jet flow reattaches on the ventricular folds where it evidences a stagnation line and initiates a well-defined recirculating flow in the Morgagni ventricle. The flow in the cavity influences the jet evolution by entrainment and by a feedback onto the instability of the jet with a time lag.

Vocal Fold Model

An existing vocal fold model is used in numerical simulation and experiment for the generation of a typical glottal jet flow. The vocal folds model used in the present study has been extensively described in [5] and is shown in Fig.1. The main physiological parameters of real vocal folds kinematics during phonation are replicated. The characteristic movement of the walls in the glottal region, e.g. the continuous deformation of the mucosal layer is achieved by means of two 3D contoured cams, which rotate in counter-direction (Fig.2). Similarity of geometry, flow dynamics and fluid dynamic forces is kept in the model. Due to very low Mach numbers, the flow is treated as incompressible.

The model is used in numerical simulations as well in experiments in a complementary way. In the experiments a pressure head across the glottal orifice is imposed. The resulting glottal volume waveform is given as input for the inlet boundary condition in the numerical model.

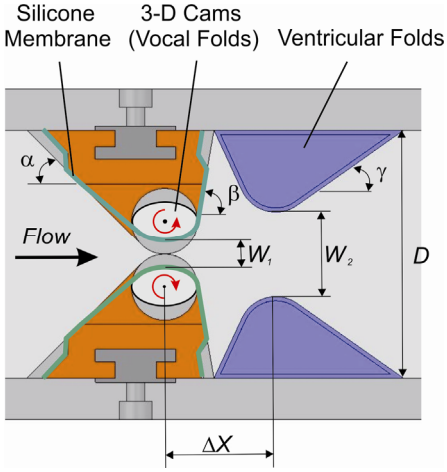

Fig.1 Midcoronal plane side view of glottal cam model: α=45°, β=80°, γ=35°, $w_2/w_{2,max}$=2.25, ΔX/D=0.4.

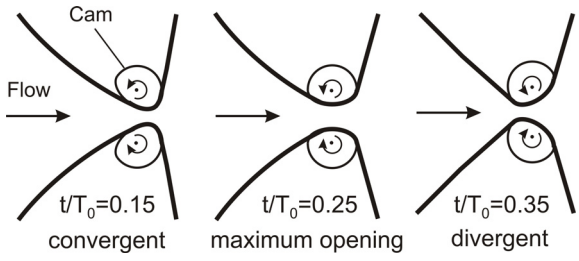

Fig.2 Characteristic open instants of the modeled glottal cycle. Instant t/T_0=0 marks the opening instant.

In the following the configurations without and with ventricular folds are denoted by (a) and (b), respectively.

Numerical Simulation

A block structured mesh of 1 million cells and with the option of evolution in time according to the dynamic glottis model is implemented. The full computational domain is shown in Fig.3.

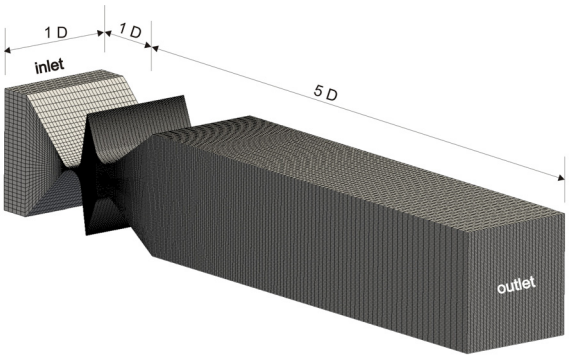

Fig.3 Computational domain.

A midcoronal plane cut-view showing the quality of the mesh in the glottal region is given in Fig.4 for a characteristic cycle instant in the closing phase.

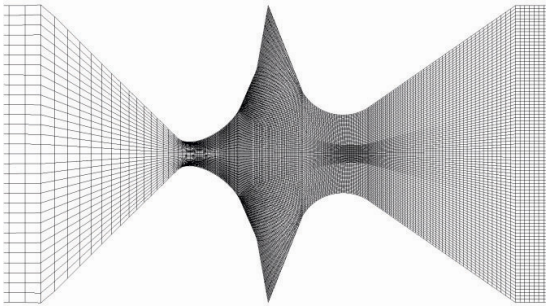

Fig.4 Example of section through glottal domain of the computational mesh for cycle instant t/T_0=0.35.

The Navier-Stokes equations for incompressible fluid flow (Eqs. (1) and (2)) are discretized with the Finite Volume method and solved numerically with the open source CFD code OpenFOAM.

$$\nabla \cdot \vec{u} = 0 \qquad (1)$$

$$\frac{\partial \vec{u}}{\partial t} + (\vec{u} \cdot \nabla)\vec{u} = -\frac{1}{\rho}\nabla p + \nu \nabla^2 \vec{u} \qquad (2)$$

The solver uses a second order Crank Nicolson time stepping and as space discretization a second order TVD scheme. The full transient 3D flow field in the near-glottal region is simulated using an implicit LES approach. In a first step time-dependent simulations have been carried out with a physiological volume waveform

synchronous to the imposed time-varying motion of the 3D glottis model. A summary of the boundary conditions is given in Tab.1.

Table 1: Boundary conditons in the simulations

boundary	Variable	type	condition
inlet	*velocity*	*Dirichlet*	$\vec{u}_{in} = \vec{u}(t)$
	pressure	*Neumann*	$\vec{n} \cdot \nabla p = 0$
outlet	*velocity*	*Neumann*	$\vec{n} \cdot \nabla \vec{u} = 0$
	pressure	*Dirichlet*	$p = 0$
wall	*velocity*	*Dirichlet*	$\vec{u}_{wall} = 0$
	pressure	*Neumann*	$\vec{n} \cdot \nabla p = 0$

A preliminary study on resolution requirements, accuracy and convergence of the model has been carried out in [6]. The experimental measurements are carried out in a test facility described in detail in Triep et al. [5].

Results

Complex 3D unsteady vortex structures are generated downstream of the glottal orifice as cause of the evolution and break-down of the glottal jet. The jet instabilities are characteristic to the instant they occur in the cycle and are linked to the time-varying 3D contour of the glottal orifice. A Kelvin-Helmholtz instability is responsible for the roll-up of the jet-edge shear layer regions.

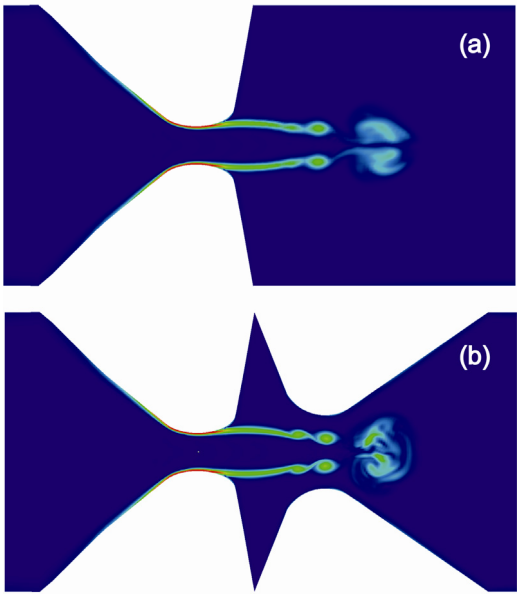

Fig.5 Regions of concentrated spanwise vorticity (absolute value normalized with maximum value) at maximum opening instant $t/T_0 = 0.25$ of the glottal cycle for both supraglottal configurations (a) and (b).

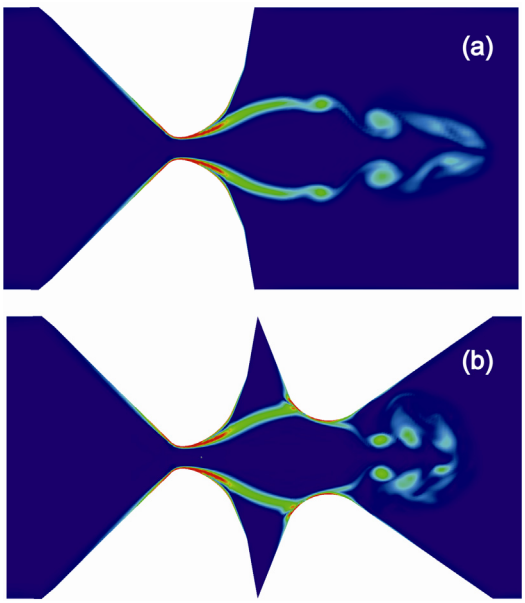

Fig.6 Regions of concentrated spanwise vorticity (absolute value normalized with maximum value) at opening instant $t/T_0 = 0.35$ of the glottal cycle for both supraglottal configurations (a) and (b).

This region of concentrated vorticity is shown in Fig.5 and Fig.6 at two distinct cycle instants $t/T_0 = 0.25$ and $t/T_0 = 0.35$. 3D flow phenomena as a lengthwise vena contracta and axis switching occur after the instant of maximum opening when the orifice is already closing.

Further flow results are shown from the numerical simulations which resolve the full 3D flow field in space and time in the glottal model. There exist several velocity or pressure based tools for vortex detection. In Fig. 7 the Q criterion [7] is used to illustrate the 3-D vortex structures. Elliptic vortex rings are generated at the glottal orifice. These are strongly deformed due to self-induction, interaction among each other and with the supraglottal walls, e.g. VFs. The complex 3D unsteady vortex structures which are generated downstream of the glottal orifice are already subjected to break-down.

In order to have a look at the near field character of the jet and study the most energetic large coherent vortex structures, mid-plane visualizations have been carried out. Fig.8 shows the experimental visualization of the flow at the maximum opening instant $t/T_0 = 0.25$ of the glottal cycle. The case without (top) and with rigid (bottom) VFs has been studied. The character of the near field of the emerging glottal jet with its most energetic large coherent vortex structures is shown. Kelvin-Helmholtz instabilities are responsible for the roll-up of the jet edge. The jet front and the successive vortex structures are seen to interact with the VFs. The determination of the pressure fluctuations due to the jet edge instabilities is given further below.

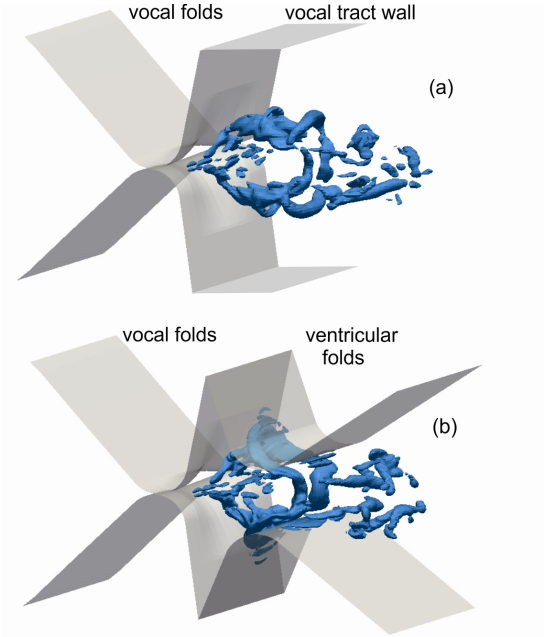

Fig.7 Representative isocontour of the Q-criterion of the flow field at the divergent closing instant $t/T_0 = 0.35$ of the glottal cycle for both supraglottal configurations (a) and (b) from Fig. 2 at the transglottal pressure of $\Delta p = 6$ cmH_2O.

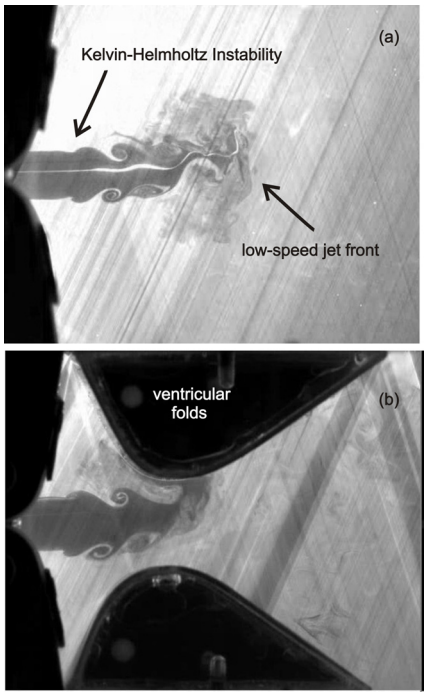

Fig.8 Visualization of the flow in the mid-coronal plane for transglottal pressure of $\Delta p = 6$ cmH_2O at maximum opening instant $t/T_0 = 0.25$ of the glottal cycle for both supraglottal configurations (a) and (b).

The distribution of the divergence of the Lamb vector **L** can be computed from the velocity **u** of the flow field and appears as a dominant acoustic source term in Lighthill's wave equation [8]. The source term reads

$$\nabla \cdot \vec{L} = \nabla \cdot ((\nabla \times \vec{u}) \times \vec{u}) \qquad (3)$$

One example of this distribution is shown in Fig. 9.

In Fig. 10 the normalized power spectra of the flow field velocity from the numerical simulation is compared for the cases without and with VFs in a center point at a downstream distance from the glottis corresponding to one vocal tract height. The differences are considerable. The change in the vortex dynamics and the spectra at different supraglottal configurations are clearly shown. A negative slope of 3 dB per octave in the low frequency range up to the 10^{th} harmonic is extracted the spectra in Fig. 5. Due to the jet edge interaction with the ventricular folds the higher frequency range of the spectrum in configuration (a) differs considerably from that in configuration (b).

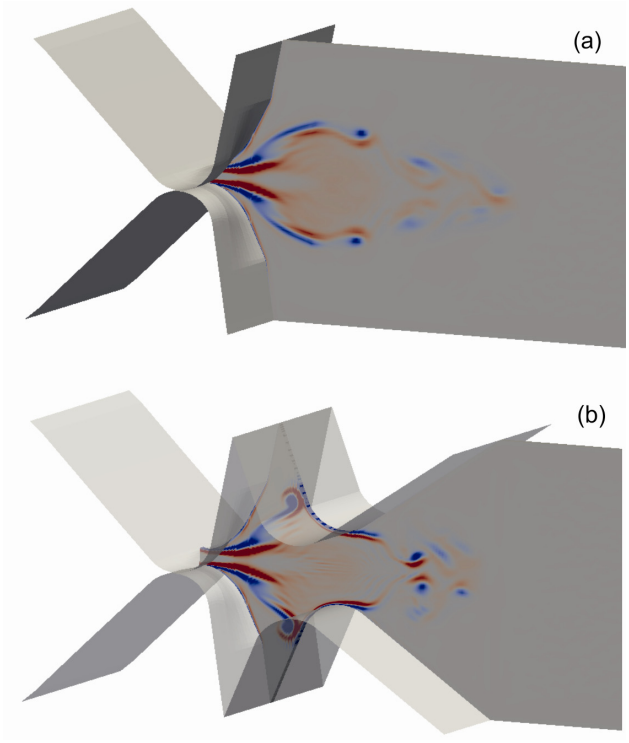

Fig.9 Distribution of the Lamb vector divergence (red positive, grey 0, blue negative value) of the flow field at the divergent closing instant $t/T_0 = 0.35$ of the glottal cycle in the mid-coronal plane for both supraglottal configurations (a) and (b) from Fig. 2.

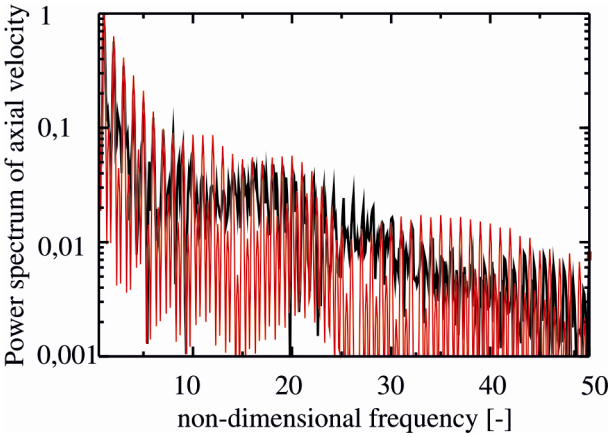

Fig.10 Power spectrum of axial velocity in a center point at distance from glottis corresponding to one vocal tract height for both supraglottal configurations (a) in black and (b) in red; Non-dimensional frequency related to fundamental frequency.

Conclusions

Results of the 3D time dependent flow field in a late instant of the glottal cycle have been shown. The comparison of the flow field in the mid-coronal plane evidences significant differences between the case where the false folds are not present with the case where these are in direct interaction with the glottal jet. The pressure fluctuations that are encountered in the glottal jet edge are influenced by these ventricular folds.

Prominent ventricular folds leave a strong fingerprint in the spectra of the flow close to the glottis. The ventricular folds redirect part of the displacement flow into the lateral gap of the Morgagni space. This built-up of a recirculation region in the gap seems to stabilize the jet core at the exit of the glottis. In addition, the shear-layer roll-up is affected by the presence of the folds and vortex structures are interacting with the walls in this region. As a consequence, vortex dynamics and wall interaction is changed considerably when supraglottal structures are included in the models. These effects are well seen in the change of spectral content within the flow. Further studies in our lab now concentrate on possible feedback and jet-control by passive and active excitation of the ventricular folds wall. Current work is focusing on the effect of flow-induced excitation of the outer layer of the false folds which is expected to enforce or dampen the higher harmonics of the glottal jet edge instabilities. This type of dynamical variation of the supraglottic geometry can have additional consequences on the non-linear feedback with the glottal jet evolution.

Acknowledgements

The authors gratefully acknowledge the support of this project by the Deutsche Forschungsgemeinschaft in the Research Group DFG FOR 894 under Contract No. Br1494/13-1. In addition, we wish to thank Mr. Clemens Kirmse for the support in the experimental measurements.

References

[1] C. Zhang, W. Zhao, S.H. Frankel and L. Mongeau, Computational aeroacoustics of phonation, Part II: Effects of flow parameters and ventricular folds, *J. Acoust. Soc. Am.* **112**, pp. 2147–2154 (2002).

[2] M. Agarwal, R.C. Scherer and K.J. De Witt, The Effects of the False Vocal Folds on Translaryngeal Airflow Resistance. Proc. *ICVPB* Marseille (2004).

[3] L. Bailly, X. Pelorson, N. Henrich and N. Ruty, Influence of a constriction in the near field of the vocal folds: Physical modeling and experimental validation, *J. Acoust. Soc. Am.* **124**, pp. 3296–3308 (2008).

[4] R.S. McGowan and M.S. Howe, Influence of the ventricular folds on a voice source with specified vocal fold motions, *J. Acoust. Soc. Am.* **127**, pp. 1519–1527 (2010).

[5] M. Triep and Ch. Brücker, Three-dimensional nature of the glottal jet, *J. Acoust. Soc. Am.* **127** , pp. 1537–1547 (2010).

[6] R. Schwarze, W. Mattheus, J. Klostermann and Ch. Brücker, Starting jet flows in a three-dimensional channel with larynx-shaped constriction, *Comp. Fluids* **48** , pp. 68–83 (2011).

[7] J.C.R. Hunt, A.A. Wray and P. Moin, Eddies, stream, and convergence zones in turbulent flows, *Center for Turbulence Research Rep. CTR-S88* (1988).

[8] M.S. Howe, Contributions to the Theory of Aerodynamic Sound, with Application to Excess Jet Noise and the Theory of the Flute, *J. Fluid Mech.* **67**, pp. 597–610 (1975).